

SUPPLEMENTARY INFORMATION for:

Enhanced Ca^{2+} influx in mechanically distorted erythrocytes: measurements with ^{19}F nuclear magnetic resonance spectroscopy

Philip W. Kuchel^{a*}, Konstantin Romanenko^a, Dmitry Shishmarev^b, Petrik Galvosas^c, and Charles D. Cox^d

^a*School of Life and Environmental Sciences, University of Sydney, Sydney, NSW, Australia*

^b*John Curtin School of Medical Research, Australian National University, Canberra, ACT, Australia.*

^c*MacDiamid Institute for Advanced Materials and Nanotechnology, School of Chemical and Physical Sciences, Victoria University Wellington, Wellington, New Zealand*

^d*Victor Chang Cardiac Research Institute, Darlinghurst, Sydney, NSW, Australia*

Supplementary Introduction

General

We provide here some context and motivation for studying Ca^{2+} and its signalling in metabolism and cell shape by using NMR spectroscopy in a way that we developed in the current project.

Calcium

Mixed phosphates and hydroxides make up ~99% of the total calcium content of the human body. It is remarkable that in the face of this huge pool, it is free Ca^{2+} *inside* cells (ionically dissociated and in the micromolar-nanomolar concentration range) that regulates metabolism, and the organization of cytoskeletal networks.

In human blood plasma, the ~ 2.2 mM Ca^{2+} is distributed as 45% free, 45% bound to protein, and 10% bound to various ligands. Again, it is the free cation in *plasma* that has various signalling roles in cells that are perfused by it [51]; *e.g.*, activation of phagocytosis in neutrophils is driven by Ca^{2+} uptake into their cytoplasm [52]. Based on extensive work, Lew and Tiffert have identified amongst other effects on RBC ionic homeostasis [53], the key role of Ca^{2+} influx in human RBCs during their senescence (and by analogy, in other mammals) [39].

Consequently, the methods developed in the present work will be valuable in exploring emerging understanding of factors that affect RBC shape, flexibility, and survival in the circulation.

Supplementary Methods

Because of the very low S/N ($\sim 4:1$) in the ^{19}F NMR spectra of RBCs loaded with 5FBAPTA, when they were suspended in gelatin, a protocol was devised to raise this to $\sim 15:1$. This meant that we forwent the aim to record spectral time courses of the influx of Ca^{2+} from one sample held in the NMR spectrometer in a 10 mm probe, over 10's of hours. Signal enhancement was ultimately achieved by removing the RBCs from the gelatin, washing them centrifugally, and recording spectra in a 5-mm NMR probe that had substantially higher sensitivity. Specifically, for a 1 M solution of $^{19}\text{F}^-$ in the 10 mm probe (glass 10-mm NMR sample tube) and the optimized (dedicated for ^{19}F) 5 mm probe the S/N was approximately the same. The 10 mm sample volume was typically 6-10 times greater than for the 5 mm probe for which the volume was much smaller, so if the same *amount* of solute were present in each sample then the optimized ^{19}F NMR probe would give ~ 6 -10 times the S/N. In addition, the RBCs in the gels had maximum packing densities of $\sim 20\%$ ($Ht = 0.2$), so extraction of them from the gel enabled the Ht to be raised four-fold to ~ 0.8 .

In addition, the washing procedure removed any extracellular 5FBAPTA-Ca complex that could have formed if there had been haemolysis, thus avoiding mis-assignment of peak area to intracellular 5FBAPTA-Ca.

Recording the spectra at 37°C , which was not feasible if retention of gel was required, meant that the extraneous $^{19}\text{F}^-$ resonance from the gelatin (Fig. S2) was also removed.

Overall, the protocol used for extracting the RBCs from compressed or stretched gels after prolonged time courses used to assess Ca^{2+} influx is shown in Fig. S1, with the various steps described in the caption.

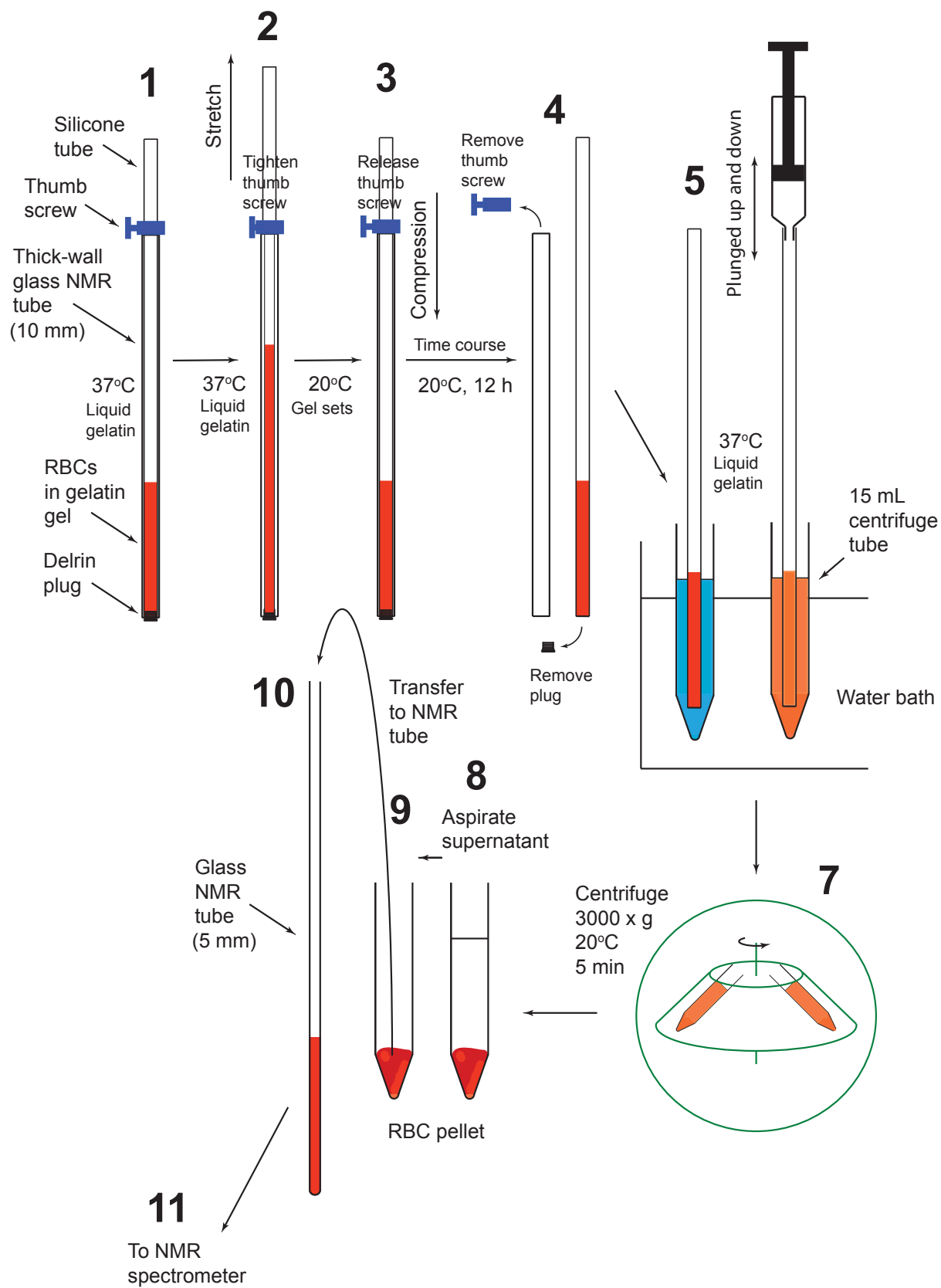


Figure S1. Experimental protocol for studying stretched (or compressed) RBCs that were extracted from the gel *prior to* ^{19}F NMR spectroscopy. The RBCs are loaded with 5FBAPTA, suspended in gelatin that was drawn into a silicone rubber tube that was held inside a glass NMR tube (**Step 1**). The silicone tube and its contents were held stretched for up to 45 h at 20°C (**Steps 2 and 3**). At the end of the time course, the sample was removed from the stretching device (**Step 4**) and then the contents of the silicone tube were extracted by melting the gel at 37°C and flushing with ~10 volumes of warm saline (**Steps 5 and 6**). The RBCs were separated from the liquid gelatin by centrifugation (**Steps 7 - 9**) including resuspension and re-centrifugation in warm saline. The RBC pellet was then transferred to a 5-mm NMR tube (**Step 10**) for acquisition of a ^{19}F NMR spectrum (**Step 11**).

Supplementary Results and Discussion

Resonance assignment to $^{19}\text{F}^-$

The relatively sharp peak at 1.53 ppm (relative to 5FBAPTA) in the ^{19}F NMR spectra shown in Fig. 2 was unexpected and demanded assignment. Assignment was made by recording a ^{19}F NMR spectrum from a sample of gelatin alone. This was done first at 20°C, the temperature used for the series of stretched and compressed RBC experiments.

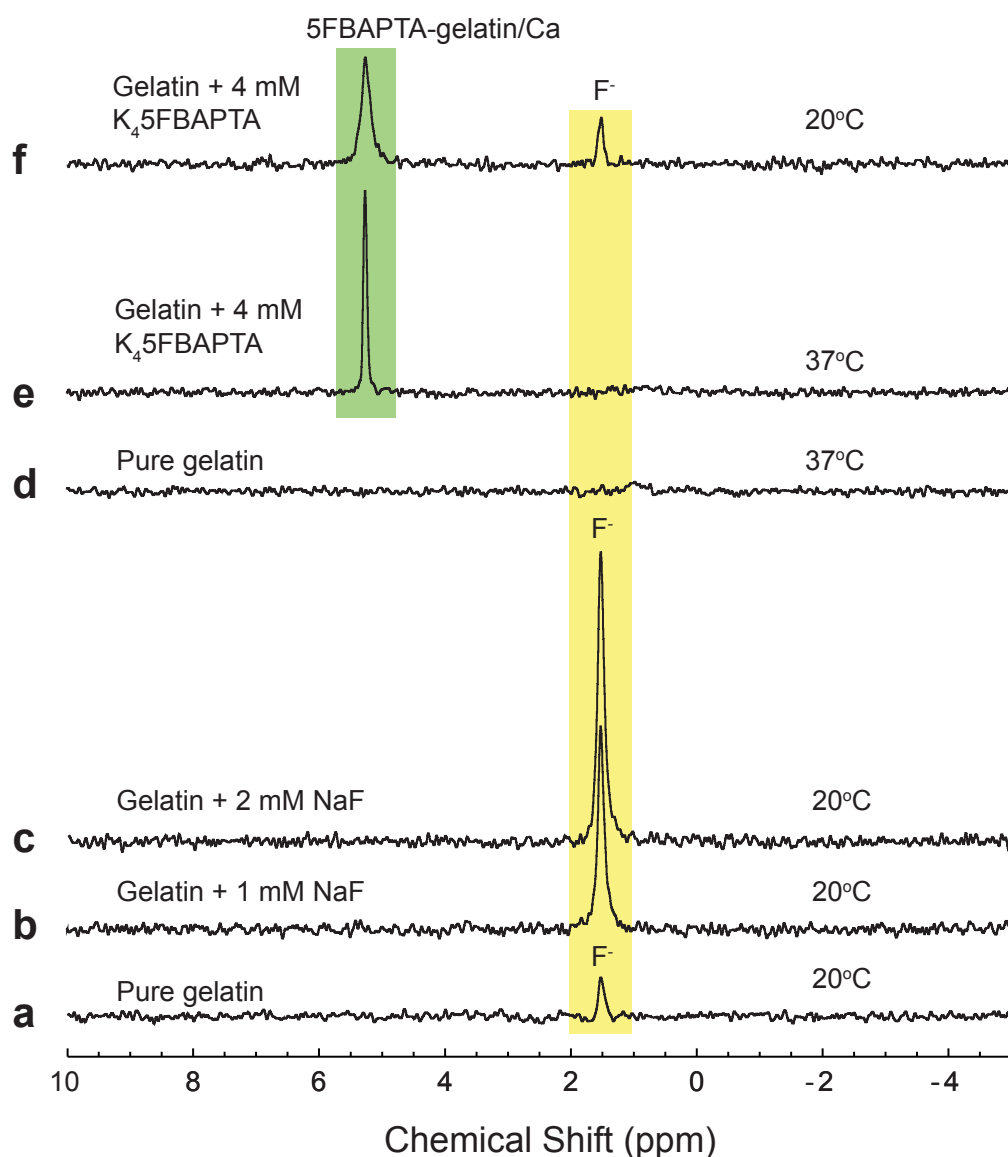


Figure S2. Assignment of the resonance at 1.53 ppm (relative to free 5FBAPTA) in ^{19}F NMR spectra of samples made up in 35% w/v Gelita gelatin, at 25°C and 37°C. Yellow highlighting on F^- ; green on 5FBAPTA-Ca complex. a, 0.7 mL sample of gelatin gel at 20°C and 37°C; d, at 37°C; b, addition 1 mM NaF to a; c, addition of extra 1 mM NaF (making 2 mM); e, 0.5 mL sample with addition of 4 mM $\text{K}_4\text{5FBAPTA}$ (10 μL of 200 mM) and ; f, sample e cooled to 20°C. NMR settings: 5-mm ^{19}F probe; total time per spectrum, 10 min; other parameters as for Fig. 6.

It is clear from Fig. S2A that the peak was present in the spectrum from pure gelatin; and that addition of NaF to the sample after it was melted at 37°C, supplemented with the NaF and then reset enhanced the peak. Further addition of NaF led to a direct quantitative increase in peak intensity, thus confirming the assignment to $^{19}\text{F}^-$. In other words, the Gelita gelatin that we used in all the experiments herein, and previously [1], is contaminated with F^- .

From the relative integrals of the spectra in Figs. S2A-C it was calculated that the concentration of $^{19}\text{F}^-$ in 35% w/v Gelita gelatin was 0.16 mol L^{-1} . This implies a ratio of amounts of $^{19}\text{F}^-$:gelatin of 27 ppm.

While food standards for levels of F^- in gelatin vary from country to country, web searching revealed that this is within acceptable limits of all recommendations reported there. In other words, our finding of a $^{19}\text{F}^-$ resonance in the ^{19}F NMR spectra of 5FBAPTA loaded RBCs in gelatin gels could have been expected; it was due to the gelatin and not to a contaminant in the 5FBAPTA-AM or in the RBCs and the various preparation media.

Resonance assignment to extracellular ^{19}F 5FBAPTA-gelatin

Figure S2E shows a spectrum from gelatin that was supplemented with 4 mM $\text{K}_4\text{5FBAPTA}$ and recorded at 37°C . Note that there was no added Ca^{2+} but the chemical shift was that of 5FBAPTA-Ca. Addition of extra Ca^{2+} (spectrum not shown) did not alter the chemical shift. When the sample from Fig. S2E was cooled to 20°C , the $^{19}\text{F}^-$ resonance appeared (as for Fig. S2A) and the peak from the $\text{K}_4\text{5FBAPTA}$ was broadened.

The latter was concluded to be due to enhanced bonding of the F-atoms on the 5FBAPTA to hydrogen bond donors on the gelatin across a distribution of sites rather than due to increased exchange with free 5FBAPTA because the temperature was lowered and not raised.

In summary: (1) gelatin contains F^- that gives a peak only when the temperature is lowered to $\sim 20^\circ\text{C}$, consistent with hydrogen bonding to gelatin's amino acid side chains; while at 37°C these bonds are weakened and exchange broadening occurs leading to loss of the peak into the baseline noise. And (2) 5FBAPTA forms hydrogen bonds with gelatin that means that its chemical shift is the same as for the complex with Ca^{2+} . Hence, if 5FBAPTA loaded RBCs in a gelatin gel rupture, a ^{19}F NMR peak that results from the release on 5FBAPTA to the extracellular medium will be due to a combination of 5FBAPTA-gelatin and 5FBAPTA-Ca and possibly also a ternary complex of both species.

Resonance assignment to extracellular ^{19}F 5FBAPTA-Ca

Figure S3A shows a ^{19}F NMR spectrum of RBCs that had been loaded with 5FBAPTA, washed with saline (154 mM NaCl) and 1% w/v BSA, and supplemented with Yoda1. There was no Ca^{2+} in this medium. The small peak at 5.9 ppm is identified as intracellular 5FBAPTA-Ca, while the adjacent sharper one at 5.5 ppm according to the argument above (Fig. S2) is from 5FBAPTA-BSA and any 5FBAPTA-Ca that would have been released by haemolysis that occurred during and after the formation of the RBC pellet.

Figure S3B was recorded after Ca^{2+} was added to the washed RBCs and it gave rise to the sharp peak at 5.5 ppm that was consistent with formation of 5FBAPTA-Ca outside the RBCs, due to haemolysis. The emergence of the broad peak at 5.9 ppm was consistent with Ca^{2+} entry via Piezo1 and the formation of intracellular 5FBAPTA-Ca with a concomitant decline in the intracellular 5FBAPTA peak at 0.0 ppm. In Figs. S3C and S3D not only did the intracellular 5FBAPTA-Ca peak grew over time, but another peak at 7.3 ppm did as well; while the sharp peak at 5.5 ppm (assigned to extracellular 5FBAPTA-Ca) did not change in intensity. The latter implies that haemolysis occurred during sample transfer to the 5-mm NMR tube and on subsequent mixing of the RBCs with the Yoda1 stock solution. The assignment of the peak at 7.3 ppm was concluded to be a ternary complex of Ca^{2+} , 5FBAPTA and intracellular protein as its growth occurred in parallel with that of 5FBAPTA-Ca, and the concomitant decline of free 5FBAPTA inside the cells.

Furthermore, addition of K45FBAPTA to the RBC suspension gave rise to a marked increase in intensity of the peak at 5.5 ppm, underscoring the veracity of the assignment of this peak to extracellular 5FBAPTA-Ca, concluded from Fig. S2. In conclusion: (1) in a simple suspension of RBCs, the sharp peak at 5.5 ppm is from extracellular 5FBAPTA-Ca; (2) in the presence of a high concentration of gelatin, this peak can also be due to 5FBAPTA-gelatin complex; (3) the peak at 5.9 ppm is from intracellular 5FBAPTA-Ca; and (4) the peak at 7.3 ppm is assigned to a ternary complex of 5FBAPTA-Ca-protein, where, based on abundance, this is likely to be haemoglobin.

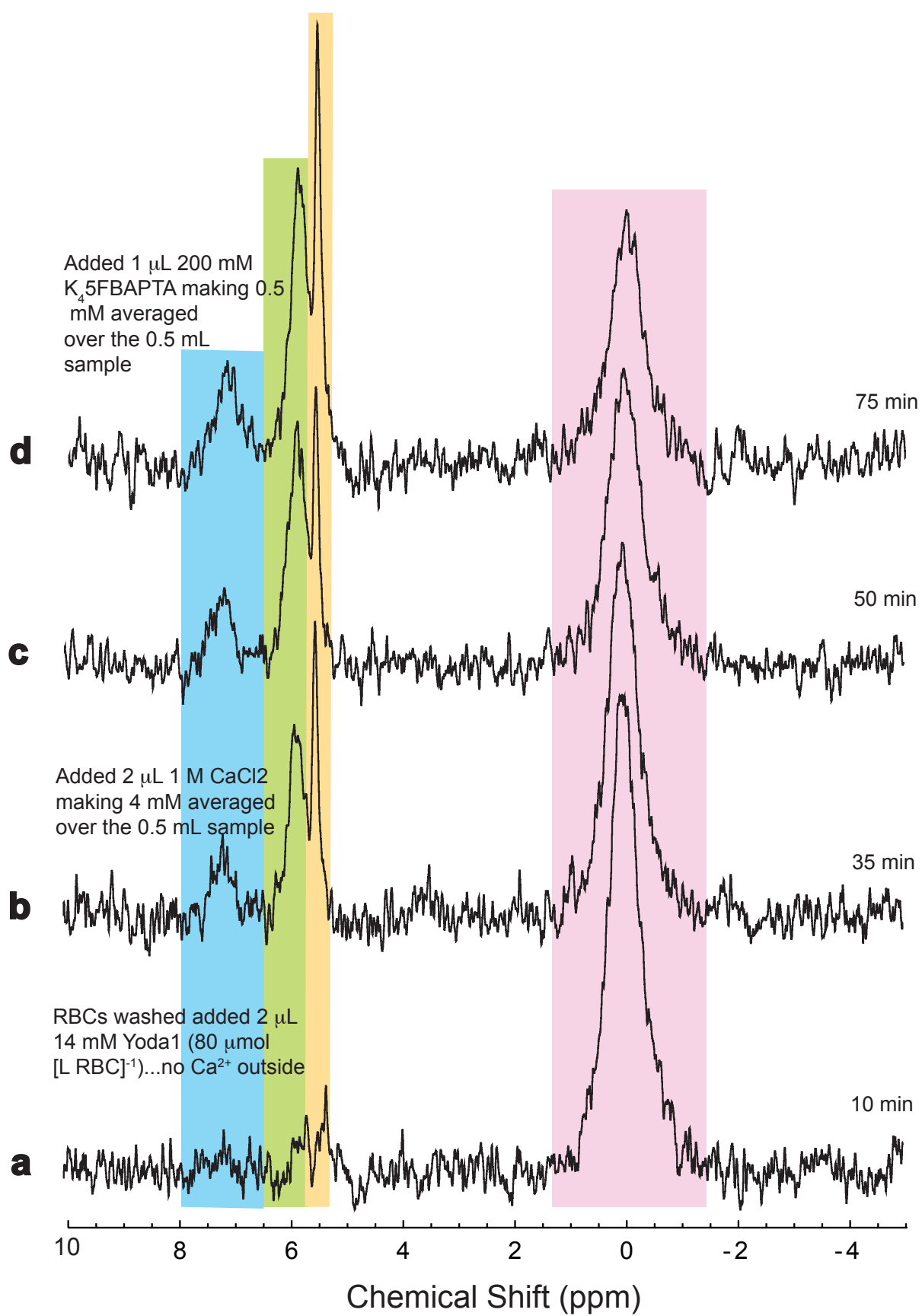


Figure S3. Assignment of ^{19}F NMR spectral peaks from 5FBAPTA and its complexes in RBC suspensions. RBCs were loaded with 3.5 mM 5FBAPTA (see Methods) and washed in physiological saline (final $Ht \sim 0.7$) that was then supplemented with $80 \mu\text{mol (L RBC)}^{-1}$ Yoda1, giving spectrum **a**. For **b**, Ca^{2+} was added to sample **a** to give 4 mM averaged over the whole sample being well in excess of the 5FBAPTA. **C** was recorded from the sample 25 min later; and then $\text{K}_4\text{5FBAPTA}$ was added (0.5 mM averaged over the sample volume) giving spectrum **d**. NMR settings: 5-mm ^{19}F probe; total time per spectrum, 10 min; other parameters as for Figure S2

^{13}C NMR of glycolysis

Figure S4 shows a ^{13}C NMR time course of spectra obtained from RBCs that had been loaded with 5FBAPTA and to which $[1,6\text{-}^{13}\text{C}]\text{D-glucose}$ was added. The insert shows the corresponding progress curve for L-lactate.

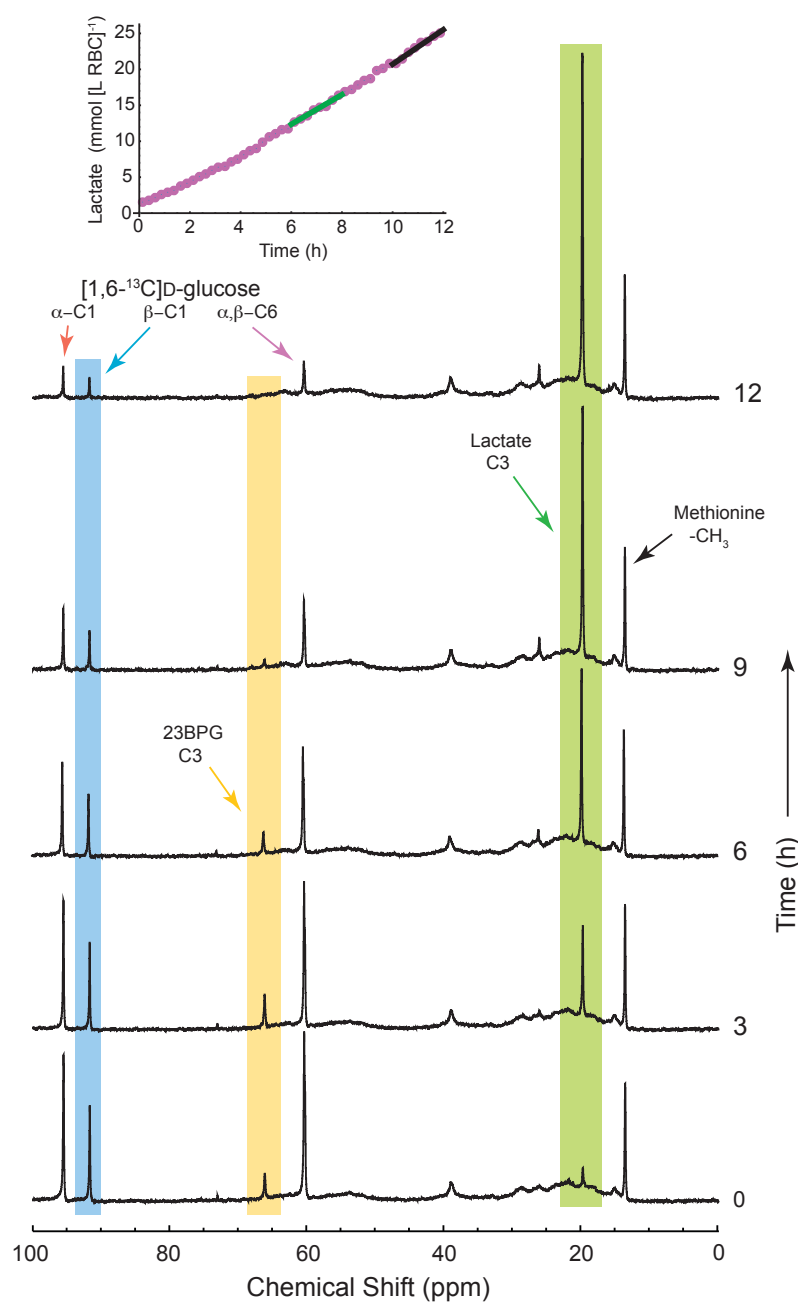


Figure S4. ^{13}C NMR (100.46 MHz) spectral time course showing glycolysis in RBCs (not loaded with 5FBAPTA) at $\sim 34^\circ\text{C}$. The control sample of 3 mL RBCs ($Ht = 0.81$) was supplemented with $[1,6-^{13}\text{C}]\text{D-glucose}$ and $^{13}\text{CH}_3\text{-L-methionine}$ (final concentrations averaged over the sample volume of 8 mM and 7 mM, respectively). Each spectrum was recorded over 15 min with only every 12th spectrum shown (centre-time of spectral acquisition time indicated on the right). The lactate resonance is highlighted in green, and the inset shows the corresponding integrals (pink dots). The black line is from linear regression onto the last eight data points (10 – 12 h; $[-3.30 \pm 1.4] + [2.40 \pm 0.13] t$) and the green line ($[0.015 \pm 0.85] + [2.06 \pm 0.12] t$) from eight points centred on 7 h. Yellow highlights the rise from an initial value and then the fall to 0 of 23BPG; and blue highlights the β -anomer of glucose that declines in parallel with the two other glucose peaks. The integral of the methionine resonance at 13.0 ppm remained constants within experimental error. The concentration of glucose, 23BPG and lactate were measured by importing the spectral data from TopSpin into a *Mathematica* program that performed automatic baseline correction and scaling to the known amount of $^{13}\text{CH}_3\text{-L-methionine}$ (that is not metabolised by human RBCs).

The progress curve shows the initial transient stage that is always seen (*e.g.*, [1]) in such experiments. It is due to the washout of unlabelled intermediates in the pentose phosphate pathway, glycolysis, and 23BPG into $^{12}\text{C-L-lactate}$. The rate of lactate production at ~ 7 h had stabilized to $2.06 \text{ mmol (L RBC)}^{-1} \text{ h}^{-1}$ and was similar 5 h later, $2.40 \pm 0.13 \text{ mmol (L RBC)}^{-1} \text{ h}^{-1}$. The time course was carried out at a setting of 30°C on the NMR-probe thermostate, but some RF heating was known to occur from trial experiments so the estimated sample temperature was $\sim 34^\circ\text{C}$. The expected rate of lactate production under the same conditions of sample preparation is $3 \text{ mmol (L RBC)}^{-1} \text{ h}^{-1}$ so the RBCs in the present study performed glycolysis normally. This was crucial to establish, because an additional feature of the preparation was inclusion of 10 mM dithioerythritol (DTE) and 1% w/v in the suspension medium. The -SH reagent was included to reduce the possibility of echinocyte formation [41] as we considered that this alone could contribute to a change in mean membrane curvature and hence stimulation of Piezo1 quite apart from mechanically induced distortion. Thus, DTE was included for the ‘Definitive’ gel-RBC stretching experiments reported in Fig. 7.